

Probing light WIMPs with directional detection experiments

Ben Morgan¹ and Anne M. Green²

¹*Department of Physics, University of Warwick, Coventry, CV4 7AL, UK*

²*School of Physics and Astronomy, University of Nottingham, University Park, Nottingham, NG7 2RD, UK*

The CoGeNT and CRESST WIMP direct detection experiments have recently observed excesses of nuclear recoil events, while the DAMA/LIBRA experiment has a long standing annual modulation signal. It has been suggested that these excesses may be due to light mass, $m_\chi \sim 5\text{--}10$ GeV, WIMPs. The Earth's motion with respect to the Galactic rest frame leads to a directional dependence in the WIMP scattering rate, providing a powerful signal of the Galactic origin of any recoil excess. We investigate whether direct detection experiments with directional sensitivity have the potential to observe this anisotropic scattering rate with the elastically scattering light WIMPs proposed to explain the observed excesses. We find that the number of recoils required to detect an anisotropic signal from light WIMPs at 5σ significance varies from 7 to more than 190 over the set of target nuclei and energy thresholds expected for directional detectors. Smaller numbers arise from configurations where the detector is only sensitive to recoils from the highest speed, and hence most anisotropic, WIMPs. However, the event rate above threshold is very small in these cases, leading to the need for large experimental exposures to accumulate even a small number of events. To account for this sensitivity to the tail of the WIMP velocity distribution, whose shape is not well known, we consider two exemplar halo models spanning the range of possibilities. We also note that for an accurate calculation the Earth's orbital speed must be averaged over. We find that the exposures required to detect 10 GeV WIMPs at a WIMP-proton cross-section of 10^{-4} pb are of order 10^3 kg day for a 20 keV energy threshold, within reach of planned directional detectors. Lower WIMP masses require higher exposures and/or lower energy thresholds for detection.

PACS numbers: 95.35.+d

I. INTRODUCTION

Direct detection experiments aim to detect dark matter in the form of Weakly Interacting Massive Particles (WIMPs) via the nuclear recoils which occur when WIMPs scatter off target nuclei [1]. The sensitivity of these experiments has increased rapidly over the last few years, and they are probing the regions of WIMP mass-cross-section parameter space populated by the lightest neutralino in Supersymmetric extensions of the standard model (see e.g. Ref. [2]).

Event rate excesses and annual modulations in various direct detection experiments have prompted recent interest in light WIMPs. The DAMA (now DAMA/LIBRA) collaboration have, for more than a decade, observed an annual modulation of the event rate in their NaI crystals [3]. This annual modulation is consistent with light ($m_\chi \sim 5\text{--}10$ GeV) WIMPs scattering off Na [4, 5]. The CoGeNT experiment, after allowing for backgrounds with an exponential plus constant energy spectrum, find an excess of low energy events which is consistent with WIMPs with mass $m_\chi \approx 7\text{--}11$ GeV [6]. With a larger data set they have observed a 2.8σ annual modulation [7], with period and phase broadly consistent with the expectation for WIMPs [8]. The CRESST experiment has observed an excess of events in their CaWO_4 crystals above expectations from backgrounds [9]. The excess is compatible with either WIMPs of mass $m_\chi \sim 25$ GeV scattering off tungsten predominantly, or lighter, $m_\chi \sim 10$ GeV, WIMPs scattering off oxygen and calcium. It appears that it is not possible to explain all of these

signals in terms of a single conventional elastic-scattering WIMP, especially when the exclusion limits from the CDMS [10], XENON10 [11] and XENON100 [12] experiments and the CRESST commissioning data [13] data are taken into account [14–16] (see also Refs. [17, 18]). None the less it is still possible that some subset of the putative signals are due to elastic scattering light WIMPs.

The deployment of a NaI detector at the South Pole has been proposed to directly test the DAMA annual modulation signal [19]. The direction dependence of the scattering rate [20] provides another potentially powerful way of testing whether the observed excesses and annual modulations are due to elastic scattering light WIMPs. The amplitude of the directional signal is far larger than that of the annual modulation and hence the anisotropy of the WIMP induced nuclear recoils could be confirmed with a relatively small number of events [21, 22]. Furthermore the angular dependence of the recoils (in particular the peak recoil rate in the direction opposite to the motion of the solar system, or for low energy recoils a ring around this direction [23]) is extremely unlikely to be mimicked by backgrounds, and would allow unambiguous detection of WIMPs [24, 25]. In this paper we investigate whether current and near future directional detectors would be able to detect elastic scattering light WIMPs.

II. MODELLING

We use the same statistical techniques and methods for calculating the directional nuclear recoil spectrum as in

Refs. [22, 26, 27]. We briefly summarise these procedures here, for further details see these references.

A. Detector

Most of the directional detectors currently under development (see Refs. [28, 29] for reviews) are low pressure gas time projection chambers (TPCs), e.g. DMTPC [30], DRIFT [31], MIMAC [32] and NEWAGE [33]. Various gases have been considered, including CF_4 , CS_2 and ^3He . We therefore consider all four of these target nuclei: ^3He , C, F and S.

Detailed calculations of the nuclear recoil track reconstruction are not available for all of these targets (see Ref. [34] for a detailed study of the reconstruction of simulated tracks for a MIMAC-like detector). Therefore we assume that the recoil directions are reconstructed perfectly in 3d. This is an optimistic assumption, therefore our results provide a lower limit on the number of events and exposure required by a real TPC based detector. Finite angular resolution does not significantly affect the number of events required to detect the anisotropic WIMP signal, provided it is not worse than of order tens of degrees [22, 35, 36]. 2d read-out would, however, significantly degrade the detector capability [22, 26, 27, 35]. We consider both vectorial and axial data i.e. where the senses of the recoils $+\mathbf{x}$ and $-\mathbf{x}$ are either measured for all recoil events or no events¹. Sense discrimination is a major challenge for directional detectors. As discussed in detail in Ref. [34], while the shape and charge distribution of nuclear recoil tracks are expected to be asymmetric, measuring these asymmetries with high efficiency is difficult in practice.

We consider four benchmark energy thresholds: $E_{\text{th}} = 5, 10, 15$ and 20 keV for each target. Note that these are directional energy thresholds. It is harder to measure the direction of a recoil than to simply detect it therefore, for a given experiment, the directional energy threshold is usually larger than the threshold for simply detecting recoils. The high energy recoils are the most anisotropic [20], therefore for heavy WIMPs a low energy threshold is not essential for directional detection. For instance for WIMPs with $m_\chi = 100$ GeV and a S target, reducing the energy threshold below 20 keV does not significantly reduce the exposure required to reject isotropy [27]. However for light WIMPs the differential event rate decreases rapidly with increasing energy, and a low threshold is crucial to obtain a non-negligible event rate. We discuss the viability of sufficiently low energy thresholds in Sec. III.

B. WIMP masses and cross-sections

We consider three benchmark light WIMP masses, $m_\chi = 5, 7.5$ and 10 GeV spanning the range of masses where the observed nuclear recoil excesses might be consistent with exclusion limits from other experiments. We fix the elastic scattering cross-section on the proton to $\sigma_p = 10^{-4}$ pb. It is straight-forward to scale our results to other values for the cross-section. The number of events required to detect anisotropy, N_{iso} , is independent of the cross-section, while the corresponding exposure, \mathcal{E} , is calculated as

$$\mathcal{E} = \frac{N_{\text{iso}}}{\sigma_p \rho R(> E_{\text{th}})}, \quad (1)$$

where $R(> E_{\text{th}})$ is the total event rate (i.e. the integral of the differential event rate) above the energy threshold normalised to unit cross-section and local WIMP density. Therefore the exposures required can be simply scaled for other cross-sections and local WIMP densities.

C. WIMP velocity distribution

The detailed angular dependence of the recoil rate depends on the exact form of the WIMP velocity distribution [21, 22, 37]. However, if the WIMP velocity distribution is dominated by a smooth component the main feature of the recoil distribution (namely the rear-front asymmetry) is robust (see e.g. Ref. [22]). The number of events required to detect anisotropy depends relatively weakly on the WIMP speed distribution [22]. However the event rate above the energy threshold, and hence the exposure required to detect anisotropy, depends more significantly on the WIMP speed distribution.

Usually the dominant uncertainty in the (time and direction averaged) differential event rate comes from the $\sim 10\%$ uncertainty [40] in the value of the local circular speed, and hence the WIMP velocity dispersion (e.g. Refs. [41–44]). The velocity dispersion and WIMP mass have somewhat degenerate effects on the differential event rate. For instance if the velocity dispersion is increased, then there are more WIMPs with higher speeds, however the energy spectra of the resulting nuclear recoils can remain the same if the WIMP mass is decreased. Therefore the range of WIMP masses corresponding to a particular observed energy spectrum excess moves to lower masses if the velocity dispersion is increased (see e.g. Ref. [17] for the specific case of CoGeNT). Varying the velocity dispersion has a qualitatively similar effect on the values of the WIMP mass consistent with the DAMA annual modulation [45]. Consequently, while varying the circular speed affects the values of the WIMP mass corresponding to, or excluded by, the various data sets, it does not significantly affect their compatibility. Therefore we fix the local circular speed to its standard value, $v_c = 220 \text{ km s}^{-1}$, consistent with our benchmark WIMP masses $m_\chi = 5, 7.5$ and 10 GeV.

¹ For studies of the effects of statistical sense determination see Refs. [36, 38].

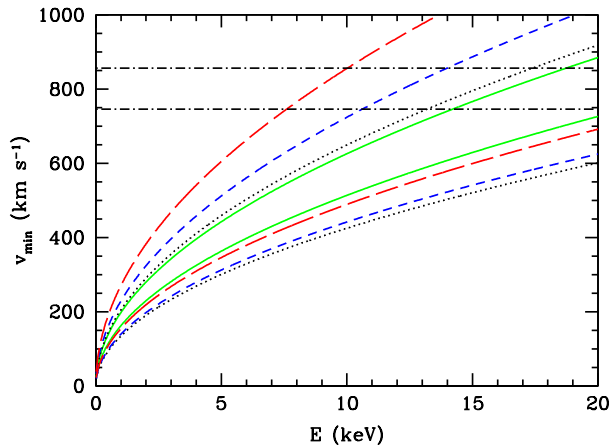


FIG. 1: The minimum WIMP speed, v_{\min} , which can cause a recoil of energy E for ${}^3\text{He}$ (solid), C (dotted), F (short dashed) and S (long dashed) for (top and bottom curves in each case respectively) $m_\chi = 5$ and 10 GeV. The horizontal dot-dashed lines show the maximum WIMP speeds in the lab, $v_\chi^{\max} \approx v_{\text{esc}} + 248 \text{ km s}^{-1}$, corresponding to the 90% upper and lower confidence limits on the escape speed from RAVE, $v_{\text{esc}}^{\max} = 608 \text{ km s}^{-1}$ and $v_{\text{esc}}^{\min} = 498 \text{ km s}^{-1}$.

Since the differential event rate involves an average over the WIMP speed distribution it is usually relatively weakly sensitive to the detailed shape of the speed distribution (e.g. Refs. [42, 46]). This is not necessarily the case, however, for experiments that are only sensitive to the high speed tail of the distribution (e.g. Refs. [43, 44, 47, 48]). The minimum WIMP speed which can cause a recoil of energy E , v_{\min} , is given by

$$v_{\min} = \left(\frac{Em_A}{2\mu_{\chi A}^2} \right)^{1/2}, \quad (2)$$

where m_A is the mass of the target nuclei and $\mu_{\chi A}$ is the reduced mass of the WIMP-target nucleus system.

Particles with speed greater than the local escape speed, $v_{\text{esc}} \equiv \sqrt{2|\Phi(R_0)|}$ where Φ is the potential and R_0 the Solar radius, will not be gravitationally bound to the Milky Way². The RAVE survey found that the escape speed lies in the range $498 \text{ km s}^{-1} < v_{\text{esc}} < 608 \text{ km s}^{-1}$ at 90% confidence, with a median likelihood of $v_{\text{esc}} = 544 \text{ km s}^{-1}$ [39]. The maximum WIMP speed in the lab frame is $v_{\text{esc}} + v_{\text{lab}}(t)$, where $v_{\text{lab}}(t)$ is the speed of the Earth with respect to the Galactic rest frame. This is made up of three components: the motion of the Local Standard of Rest (LSR), $\mathbf{v}_{\text{LSR}} = (0, v_c, 0)$ in Galactic coordinates, the Sun's peculiar motion with respect to the LSR, $\mathbf{v}_\odot^p(11.1, 12.2, 7.3) \text{ km s}^{-1}$ [50], and the Earth's

orbit about the Sun, $\mathbf{v}_e^{\text{orb}}(t)$. It has a maximum value at $t_0 \approx 153$ days (on June 2nd) of $v_{\text{lab}}^{\max} = v_{\text{lab}}(t_0) \approx 248 \text{ km s}^{-1}$.

Fig. 1 shows v_{\min} as a function of E for $m_\chi = 5$ and 10 GeV for ${}^3\text{He}$, C, S and F target nuclei. The horizontal lines show the maximum WIMP speeds in the lab, $v_\chi^{\max} = v_{\text{esc}} + v_{\text{lab}}^{\max}$, corresponding to the 90% upper and lower confidence limits on the escape speed from RAVE, $v_{\text{esc}}^{\max} = 608 \text{ km s}^{-1}$ and $v_{\text{esc}}^{\min} = 498 \text{ km s}^{-1}$. For light WIMPs, unless the target nuclei are light and the threshold energy low, the minimum speed corresponding to the threshold energy lies in the tail of the speed distribution, and in some cases beyond the cut-off due to the Galactic escape speed. The expected event rates are therefore very sensitive to the value of the escape speed and the shape of the high speed tail of the distribution.

The standard halo model, an isotropic, isothermal sphere with density profile $\rho(r) \propto r^{-2}$, is formally infinite. Hence its Maxwellian velocity distribution,

$$f(\mathbf{v}) = N \exp\left(-\frac{3|\mathbf{v}|^2}{2\sigma^2}\right), \quad (3)$$

where $\sigma = \sqrt{3/2}v_c$ and N is a normalisation constant, extends to infinity too. This is usually addressed by truncating the velocity distribution by hand, either sharply or exponentially, at the escape speed.

Numerical simulations find velocity distributions with less high speed particles than the standard Maxwellian [51–53]. Lisanti et al. [47] have presented an ansatz for the velocity distribution which reproduces this behaviour:

$$f(|\mathbf{v}|) \propto \left[\exp\left(\frac{v_{\text{esc}}^2 - |\mathbf{v}|^2}{kv_0^2}\right) - 1 \right]^k \Theta(v_{\text{esc}} - |\mathbf{v}|). \quad (4)$$

The parameter k is related to the outer slope of the density profile, γ , ($\rho(r) \propto r^{-\gamma}$ for large r), by $k = \gamma - 3/2$ for $\gamma > 3$ [54].

We consider 2 forms for $f(\mathbf{v})$ chosen to have high speed tails which roughly span the plausible range. Firstly, a Maxwellian distribution, eq. (3), with a sharp cut-off ($f(\mathbf{v}) = 0$ for $|\mathbf{v}| \geq v_{\text{esc}}^{\max}$) at the upper limit on the escape speed from RAVE, $v_{\text{esc}}^{\max} = 608 \text{ km s}^{-1}$, which provides a large tail event rate. Secondly, a Lisanti et al. $f(v)$, eq. (4), with $v_{\text{esc}} = v_{\text{esc}}^{\min} = 498 \text{ km s}^{-1}$ to provide a small tail event rate. We fix $k = 1.5$, corresponding to an outer density profile slope $\gamma = 3$ and $v_0 = v_c = 220 \text{ km s}^{-1}$. In both cases we fix the local density to be $\rho = 0.3 \text{ GeV cm}^{-3}$. Scaling the event rates and exposures to other densities is straight-forward.

Fig. 2 shows the differential event rates for each of the WIMP masses and targets we consider calculated using the Maxwellian distribution with a sharp cut-off at $v_{\text{esc}}^{\max} = 608 \text{ km s}^{-1}$. The much smaller event rates for He are largely due to the A^2 factor in the event rate for spin-independent scattering. For heavier targets the differential event rate in the $E \rightarrow 0$ limit is substantially larger, however it decreases rapidly with increasing E ,

² Dark matter halos do contain unbound particles, however the fraction of such particles at the Solar radius is small [49].

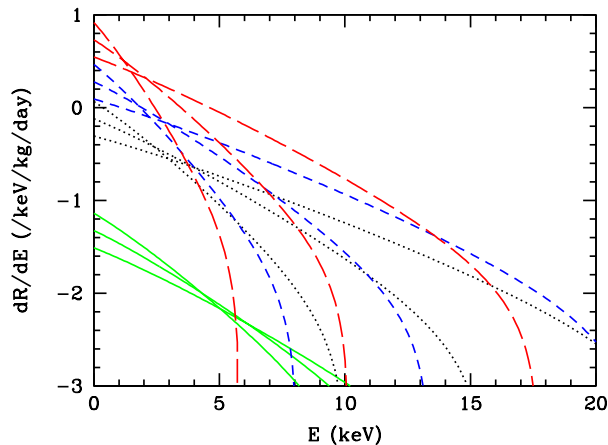


FIG. 2: The differential event rates, assuming a Maxwellian speed distribution with a sharp cut-off at $v_{\text{esc}}^{\text{max}} = 608 \text{ km s}^{-1}$, a cross-section $\sigma_p = 10^{-4} \text{ pb}$ and a local WIMP density $\rho = 0.3 \text{ GeV cm}^{-3}$, for He (solid), C (dotted), F (short dashed) and S (long dashed) for (from top to bottom at $E = 0 \text{ keV}$) $m_\chi = 5, 7.5$ and 10 GeV .

and the lighter the WIMP the more rapid the decrease. Furthermore for relatively small energies v_{min} exceeds the maximum WIMP speed in the lab frame and hence the differential event rate is zero.

Fig. 3 shows the ratio of the speed integral,

$$g(v_{\text{min}}) = \int_{v_{\text{min}}}^{\infty} \frac{f(v)}{v} dv, \quad (5)$$

for Lisanti et al.'s $f(v)$ in eq. (4) with $v_{\text{esc}}^{\text{min}} = 498 \text{ km s}^{-1}$ to that for the Maxwellian distribution with a sharp cut-off at $v_{\text{esc}}^{\text{max}} = 608 \text{ km s}^{-1}$. It also shows the velocity integral ratios for these two models if the Earth's orbit is neglected. For $v_{\text{min}} \lesssim \mathcal{O}(300 \text{ km s}^{-1})$ the difference in the speed integrals for the two speed distributions is relatively small, less than 10%. As v_{min} is increased, so that only the tail of the speed distribution is included in the speed integral, the difference becomes substantially larger, reaching roughly an order of magnitude for $v_{\text{min}} \sim 650 \text{ km s}^{-1}$. Neglecting the Earth's orbit has a significant ($> 10\%$) effect, for v_{min} within $\sim 100 \text{ km s}^{-1}$ of the maximum WIMP speed in the lab frame v_χ^{max} . Therefore the Earth's orbital speed must be included, and averaged over, for an accurate calculation of the event rate.

Simulated dark matter halos have velocity distributions which contain features at high speeds [52, 53]. More specifically there are fairly broad features, which are similar at different positions within a single halo, but which vary from halo to halo, and are hence thought to be a relic of the formation history of the halo [52, 53, 55]. Ref. [53] also finds narrow features in some locations, corresponding to tidal streams, while Ref. [56] finds that the dark matter streams from the Sagittarius dwarf are significantly more extended than the stellar streams, and the

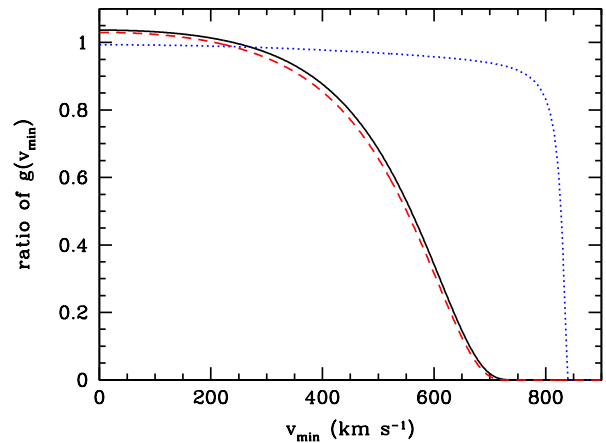


FIG. 3: The speed integral, $g(v_{\text{min}})$, relative to that for the Maxwellian distribution with a sharp cut-off at $v_{\text{esc}}^{\text{max}} = 608 \text{ km s}^{-1}$, including averaging over the Earth's orbit. The solid line is for Lisanti et al.'s $f(v)$, eq. (4), with $v_{\text{esc}}^{\text{min}} = 498 \text{ km s}^{-1}$, including the Earth's orbit. The dotted and dashed lines are for the Maxwellian and Lisanti et al. distributions respectively, neglecting the Earth's orbit.

leading dark matter stream may pass through the Solar neighbourhood. The detailed shape of the high speed tail of $f(v)$ would affect the interpretation of the CoGeNT, CRESST and DAMA data, in particular the values of the WIMP mass extracted. Since no detailed study of this has been carried out to date³, we do not include the high speed features in our analysis. We defer a general investigation of the directional event rate produced by simulation velocity distributions to future work [58].

D. Statistical tests

We follow the statistical procedures described in detail in Refs. [22, 27]. We use the Rayleigh-Watson statistic, which uses the mean resultant length of the recoil direction vectors. We also use the Bingham statistic which, unlike the Rayleigh-Watson statistic, can be used with axial data (where the senses of the nuclear recoils are not measured). These statistics are described in more detail in Appendices A and B.

For each WIMP mass, target nuclei and energy threshold combination we calculate the probability distribution of each statistic for WIMP induced recoils and also for the null hypothesis of isotropic recoils. We use these distributions to calculate the rejection and acceptance

³ Ref. [15] includes tidal streams with specific properties chosen to reproduce the energy dependence of the amplitude of the annual modulation measured by CoGeNT, while Ref. [57] studies the effects of the Sagittarius tidal stream.

factors, R and A . The rejection factor gives the confidence level with which the null hypothesis can be rejected given a particular value of the test statistic, while the acceptance factor is the probability of measuring a larger value of the test statistic if the alternative hypothesis is true. We then find the number of events required for $A = R = 0.95, 0.99730$ and 0.999999427 i.e. to reject isotropy at this confidence level in this percentage of experiments (see Refs. [22, 27] for further discussion). The later two confidence levels correspond, for a gaussian distribution, to three and five sigma respectively. Since our aim is to examine whether directional detection experiments could detect light WIMPs we will focus on the case $A = R = 0.999999427$, corresponding to the ‘five sigma’ result conventionally required for discovery.

III. RESULTS AND DISCUSSION

For each of the combinations of WIMP mass, target nuclei, energy threshold and confidence level discussed in Sec. II we calculate the number of events required to reject isotropy, N_{iso} , for vector and axial data (using the Rayleigh-Watson and Bingham statistics respectively). The number of events required for a 5σ detection with the Rayleigh-Watson statistic varies from 7 to 58. For fixed WIMP and target mass, N_{iso} decreases with increasing energy threshold, E_{th} , (since the recoils caused by high speed WIMPs in the tail of the distribution are more anisotropic), until the minimum speed required to cause a recoil of energy E_{th} , $v_{\text{min}}(E_{\text{th}})$, exceeds the maximum WIMP speed in the lab frame, v_{χ}^{max} . At this point the event rate is zero and no events can be detected. The same trend occurs for decreasing WIMP mass (with threshold energy and target mass fixed). For fixed threshold energy, N_{iso} decreases with increasing target mass for $m_{\chi} = 5$ GeV, however for $m_{\chi} = 7.5$ and 10 GeV, N_{iso} increases as the target mass number is increased from $A = 3$ to 12 before decreasing as A is increased further. This is due to the variation of v_{min} with target and WIMP mass shown in Fig. 1.

For the Bingham statistic, which can be used with axial data, the number of events required for a 5σ detection varies from 9 to more than 190⁴. Both the number of events and its increase, relative to the number required for the Rayleigh-Watson statistic, is smallest for the configurations which are only sensitive to the highly anisotropic recoils from high speed WIMPs in the tail of the speed distribution.

If an experiment is only sensitive to high speed WIMPs, fewer events are required to reject isotropy, however, the reduced event rate means that the exposure re-

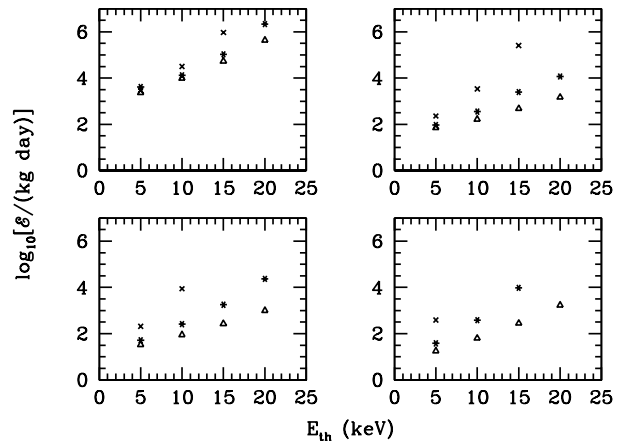


FIG. 4: The exposure required for a 5σ rejection of isotropy as a function of energy threshold, E_{th} , for ${}^3\text{He}$ (top left), C (top right), F (bottom left) and S (bottom right) for $m_{\chi} = 5, 7.5$ and 10 GeV (crosses, stars and triangles respectively) for the Maxwellian $f(v)$ with a sharp cut-off at $v_{\text{esc}}^{\text{max}} = 608 \text{ km s}^{-1}$. Where a symbol is not displayed, the minimum WIMP speed corresponding to the energy threshold, $v_{\text{min}}(E_{\text{th}})$, for this WIMP and target mass combination exceeds the maximum WIMP speed in the lab frame, v_{χ}^{max} and hence the event rate is zero.

quired to accumulate these events will be larger. We therefore use eq. (1) to calculate the exposure, \mathcal{E} , (in kg day) required to accumulate the required number of events for each case. As illustrated in Fig. 2, for light WIMPs the differential event rate decreases rapidly with increasing energy, and therefore the event rate above the energy threshold, $R(> E_{\text{th}})$, plays a crucial role in determining the exposure required.

The exposure required to reject isotropy at 5σ using the Rayleigh-Watson statistic assuming a Maxwellian $f(v)$ with a sharp cut-off at $v_{\text{esc}}^{\text{max}} = 608 \text{ km s}^{-1}$ is shown for each configuration in Fig. 4. While N_{iso} varies by less than an order of magnitude, because of the large variation in $R(> E_{\text{th}})$, the exposure varies by more than five orders of magnitude. Due to the rapid decrease of $R(> E_{\text{th}})$, the exposure increases sharply with increasing E_{th} for each WIMP and target nuclei mass combination. The factor by which the exposure increases, increases with both decreasing WIMP mass and increasing target nuclei mass (i.e. as the minimum WIMP speed to which the experiment is sensitive is increased). Eventually the minimum WIMP speed corresponding to the energy threshold, $v_{\text{min}}(E_{\text{th}})$, exceeds the maximum WIMP speed in the lab frame, v_{χ}^{max} , and the event rate is zero and WIMPs of this mass can not be detected.

Of the halo models considered, the Maxwellian $f(v)$ with a sharp cut-off at $v_{\text{esc}}^{\text{max}} = 608 \text{ km s}^{-1}$ has the largest tail event rate, and hence the smallest exposures. In Fig. 5 we show the exposures for a S target for the Lisanti et al. $f(v)$, eq. (4), with $v_{\text{esc}}^{\text{min}} = 498 \text{ km s}^{-1}$ as well. When $v_{\text{min}}(E_{\text{th}})$ is much smaller than v_{χ}^{max} the expo-

⁴ In a small number of cases, where a large number of events are required, we have only been able to place a lower limit on N_{iso} due to computational time limitations.

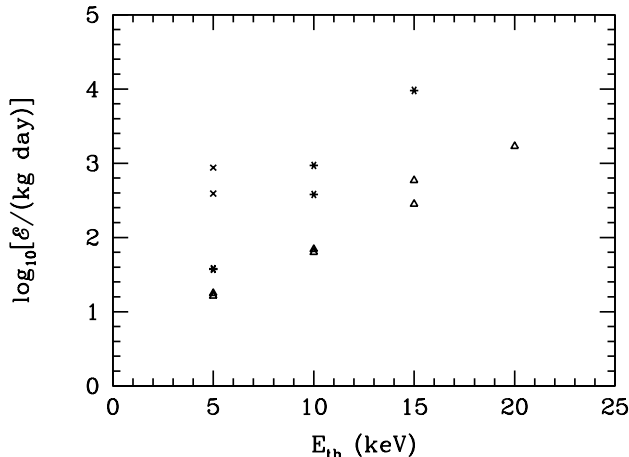


FIG. 5: As Fig. 4 but for a S target only comparing the exposures required for the Lisanti et al. $f(v)$, eq. (4), with $v_{\text{esc}}^{\text{min}} = 498 \text{ km s}^{-1}$ (upper symbols) with those for the Maxwellian $f(v)$ with a sharp cut-off at $v_{\text{esc}}^{\text{max}} = 608 \text{ km s}^{-1}$ (lower symbols). For $m_\chi = 7.5 \text{ keV}$ and $E_{\text{th}} = 5 \text{ keV}$ the exposures required for the two speed distributions are the same, and hence only one symbol is visible.

sure required is fairly modest, $\mathcal{E} \sim 10 - 100 \text{ kg day}$ and the event rates, and hence exposures, for the two speed distributions are very similar. However as $v_{\text{min}}(E_{\text{th}})$ approaches v_χ^{max} the exposures required become large and the differences between the two speed distributions become significant. For instance for $E_{\text{th}} = 20 \text{ keV}$, WIMPs with $m_\chi = 10 \text{ GeV}$ and a Maxwellian distribution with $v_{\text{esc}}^{\text{max}} = 608 \text{ km s}^{-1}$ anisotropy could be detected with an exposure of 1700 kg day , however if the WIMPs have the Lisanti et al. $f(v)$ with $v_{\text{esc}}^{\text{min}} = 498 \text{ km s}^{-1}$ the event rate is zero and they can not be detected. The trends for the other target nuclei are similar.

In Fig. 6 we compare the exposures required to reject isotropy with axial data using the Bingham statistic with those for vectorial data using the Rayleigh-Watson statistic, for a S target and a Maxwellian $f(v)$ with a sharp cut-off at $v_{\text{esc}}^{\text{max}} = 608 \text{ km s}^{-1}$. Since $R(> E_{\text{th}})$ for each configuration doesn't change, the variations in the exposure are driven entirely by the variations in N_{iso} discussed above. Therefore the increase in the exposure, relative to that required for the Rayleigh-Watson statistic, is smallest for the cases which are only sensitive to the highly anisotropic recoils from high speed WIMPs in the tail of the speed distribution. However in these cases the exposure is large even for the Rayleigh-Watson statistic, due to the small values of $R(> E_{\text{th}})$.

We have focused on the number of events and exposure required for a '5 σ ' discovery of light WIMPs with a directional detector. Significant experimental support for light WIMPs would be obtained even with a lower significance signal. For 95% and 99.713% confidence levels (the later corresponding to 3 σ) the number of events, and hence the exposure, required with the Rayleigh-Watson

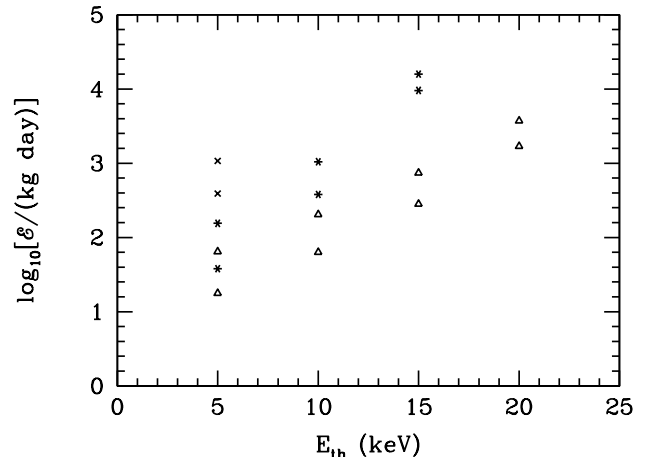


FIG. 6: As Fig. 5 but comparing the exposures required using the Bingham statistic (upper symbols) with those required using the Rayleigh statistic (lower symbols), in both cases for a S target using a Maxwellian $f(v)$ with a sharp cut-off at $v_{\text{esc}}^{\text{max}} = 608 \text{ km s}^{-1}$. For $m_\chi = 10 \text{ GeV}$ and $E_{\text{th}} = 5 \text{ keV}$ we have only been able to place a lower bound on the number of events, and hence exposure, required with the Bingham statistic.

statistic is smaller by a factor of between $0.40 - 0.91$ and $0.69 - 0.95$ respectively. The factor by which the number of events must be increased to increase the significance of the rejection of isotropy is smallest when the experiment is only sensitive to the most anisotropic events coming from the tail of the speed distribution. However in these cases the exposure required even for a low significance detection is large.

The final question is 'How achievable are these exposures and energy thresholds by current and near-future detectors?' A typical current detector consisting of a 1 m^3 TPC filled to 75 Torr with CF_4 or CS_2 could, in roughly a year, achieve an exposure of order 10^3 kg day [29]. A 10^3 kg day exposure with CF_4 or CS_2 would (provided that recoils are measured in 3d with good, $\lesssim 10^\circ$, angular resolution) be capable of detecting $m_\chi = 10 \text{ keV}$ WIMPs with an energy threshold of 20 keV or lower. Lighter WIMPs would require a lower energy threshold, potentially as low as 5 keV for $m_\chi = 5 \text{ GeV}$. With a ^3He target a low, $\sim 5 \text{ keV}$, energy threshold would be required, even for $m_\chi = 10 \text{ GeV}$. Measuring the directions of low energy nuclear recoils is a major experimental challenge, and these energy threshold are lower than those which have been used in the analysis of data from current, prototype, detectors [29]. One of the focuses of the R&D for future generation experiments is to reduce the energy threshold (see e.g. [59]). The MIMAC experiment has, using micromegas readout, detected 5 keV F recoils [60], while DRIFT-II is sensitive to nuclear recoils down to sub 5 keV energies [61]. Simulations of the MIMAC detector indicate that the directional energy threshold will lie below 20 keV [34]

IV. SUMMARY

The event rate excess and annual modulations observed by various direct detection experiments may be due to light, 5 – 10 GeV WIMPs. We have investigated whether near future directional detection experiments will be able to test this possibility, by detecting the anisotropy of the nuclear recoils. We find, using the Rayleigh-Watson statistic, that an ideal directional detector (capable of measuring the directions of the recoils, including their senses, in 3d with good angular resolution) would require between 7 and 58 events to detect the anisotropy at 5σ . The number of events required depends on the target nuclei mass, energy threshold, WIMP mass, and crucially the details of the high speed tail of the WIMP speed distribution. It is smallest for cases where the experiment is only sensitive to the highly anisotropic recoils from high speed WIMPs in the tail of the speed distribution. If the detector is not capable of measuring the senses of the recoils we find, using the Bingham statistic, that the number of events required ranges between 9 and more than 190. The increase in the number of events required with axial data is smallest for the cases which are only sensitive to high speed WIMPs due to the higher degree of anisotropy in the nuclear recoil distributions.

In terms of the detection potential the key quantity is the exposure necessary to detect the required number of events, which is inversely proportional to the event rate above threshold. For the configurations we have considered (^3He , C, F and S targets, 5 – 10 GeV WIMPs and energy threshold between 5 and 20 keV) the event rate above threshold varies by more than five orders of magnitude, and in some cases the minimum speed required to cause a recoil above threshold exceeds the maximum WIMP speed in the lab and the event rate is zero. For the cases which are only sensitive to high speed WIMPs, where the number of events required was smallest, the event rate above threshold is small and hence very large exposures would be required. The shape of the high speed tail of the WIMP distribution is not well known and this leads to large uncertainties in the event rate expected in experiments which are only sensitive to the high speed tail, c.f. Refs. [43, 44, 47, 48]. We also emphasize that including, and averaging over, the Earth's orbit is essential for an accurate calculation of the event rate in these cases.

We find that a future CF_4 or CS_2 detector with an energy threshold of 20 keV or lower, which can measure recoil directions and senses in 3d with good angular resolution, would be capable of detecting WIMPs with $(m_\chi, \sigma_p) = (10 \text{ GeV}, 10^{-4} \text{ pb})$ with an exposure of 10^3 kg day . Detecting lighter WIMPs would require a lower energy threshold. With a ^3He target a low, $\sim 5 \text{ keV}$, energy threshold would be required, even for WIMP masses at the upper end of the mass range considered. In summary, we conclude that directional detection experiments may be able to detect light WIMPs, but this depends quite sensitively on both the experimental

configuration (target nuclei mass and energy threshold) and the unknown WIMP mass and velocity distribution. The directional energy thresholds required to detect light WIMPs are below those used in analyses of data from current directional detectors, however it has been demonstrated that directional detectors can detect [60, 61] and measure the directions [34] of low energy nuclear recoils and R&D is underway to realise lower energy thresholds [59].

We also note that directional experiments, with heavy targets, could also test inelastic dark matter as the explanation of the direct detection anomalies [62].

Acknowledgments

AMG and BM are supported by STFC.

Appendix A: Rayleigh Watson statistic

The (modified) Rayleigh-Watson statistic, \mathcal{W}^* is the simplest coordinate independent statistic for detecting anisotropy in vectorial data. It is related to the Rayleigh statistic, \mathcal{R} , which for a sample of N unit vectors \vec{x}_i is given by

$$\mathcal{R} = \left| \sum_{i=1}^N \vec{x}_i \right|. \quad (\text{A1})$$

i.e. the modulus of the sum of vectors. For an isotropic data set \mathcal{R} should be zero, modulo statistical fluctuations. For anisotropic data the value of \mathcal{R} becomes larger as the degree of anisotropy increases.

The modified Rayleigh-Watson statistic, \mathcal{W}^* , defined as [63–65]

$$\mathcal{W}^* = \left(1 - \frac{1}{2N}\right) \mathcal{W} + \frac{1}{10N} \mathcal{W}^2, \quad (\text{A2})$$

where \mathcal{W} is the (unmodified) Rayleigh-Watson statistic

$$\mathcal{W} = \frac{3}{N} \mathcal{R}^2. \quad (\text{A3})$$

The modified statistic \mathcal{W}^* has the advantage of approaching its large N asymptotic distribution for smaller N than the unmodified statistic. For isotropically distributed vectors, \mathcal{W}^* is asymptotically distributed as χ_3^2 [63, 64]. The difference between χ_3^2 and the true distribution of \mathcal{W}^* for isotropic vectors in the large \mathcal{W}^* tail of the distribution is less than 2% for $N > 30$ [22]. For smaller N the χ_3^2 distribution significantly underestimates the true probability distribution and therefore, as in Ref. [22] we calculate the probability distribution from the exact probability distribution of \mathcal{R} , as described in Ref. [66].

Appendix B: Bingham statistic

The Rayleigh-Watson statistic can not be used with axial data, as it is not sensitive to distributions which are symmetric with respect to the centre of the sphere. For axial data the Bingham statistic \mathcal{B}^* which is based on the scatter matrix of the data, \mathbf{T} , can be used. This matrix is defined as [64, 65, 67]

$$\mathbf{T} = \frac{1}{N} \sum_{i=1}^N \begin{pmatrix} x_i x_i & x_i y_i & x_i z_i \\ y_i x_i & y_i y_i & y_i z_i \\ z_i x_i & z_i y_i & z_i z_i \end{pmatrix}, \quad (\text{B1})$$

where (x_i, y_i, z_i) are the components of the i -th vector or axis. This matrix is real and symmetric with unit trace,

so that the sum of its eigenvalues e_k ($k = 1, 2, 3$) is unity, and for an isotropic distribution all three eigenvalues should, modulo statistical fluctuations, be equal to $1/3$. The Bingham statistic, \mathcal{B} ,

$$\mathcal{B} = \frac{15N}{2} \sum_{k=1}^3 \left(e_k - \frac{1}{3} \right)^2, \quad (\text{B2})$$

measures the deviation of the eigenvalues e_k from the value of $1/3$ expected for an isotropic distribution. For isotropically distributed vectors/axes \mathcal{B} is asymptotically distributed as χ_5^2 . Since \mathbf{T} is symmetric under a sign change of \vec{x} , the Bingham statistic can be used for axial data as well as vectors.

-
- [1] M. W. Goodman and E. Witten, Phys. Rev. D **31**, 3059 (1985).
- [2] B. Bertone, D. G. Cerdeno, M. Fornasa, R. Ruiz de Austri, C. Strece and R. Trotta, JCAP01(2012)015, arXiv:1107.1715.
- [3] R. Bernabei et al., Eur. Phys. C **56**, 39 (2010), arXiv:1002.1028.
- [4] A. Bottino, F. Donato, N. Fornengo and S. Scopel, Phys. Rev. D **69** (2004) 037302 [hep-ph/0307303].
- [5] G. B. Gelmini and P. Gondolo, Phys. Rev. D **74** 123520 (2005), arXiv:0504010.
- [6] C. E. Aalseth et al., Phys. Rev. Lett. **106**, 131301 (2011), arXiv:1002.4703.
- [7] C. E. Aalseth et al., Phys. Rev. Lett. **107**, 141301 (2011), arXiv:1106.0650.
- [8] A. K. Drukier, K. Freese and D. N. Spergel, Phys. Rev. D **33**, 3495 (1986).
- [9] G. Angloher et al., Eur. Phys. J. C **72**, 1971 (2012), arXiv:1109.0702.
- [10] D. S. Akerib et al., Phys. Rev. D **82**, 122004 (2010), arXiv:1010.4290.
- [11] J. Angle et al., Phys. Rev. Lett. **107** 051301 (2011), arXiv:1104.3088.
- [12] E. Aprile et al., Phys. Rev. Lett. **107** 131302 (2011), arXiv:1104.2549; arXiv:1207.5988.
- [13] A. Brown, S. Henry, H. Kraus and C. McCabe, Phys. Rev. D **85**, 021301 (2012), arXiv:1109.2589.
- [14] J. Kopp, T. Schwetz and J. Zupan, JCAP03(2012)001, arXiv:1110.2721.
- [15] C. Kelso, D. Hooper and M. R. Buckley, Phys. Rev. D **85** 043515 (2012), arXiv:1110.5338.
- [16] M. T. Frandsen, F. Kahlhoefer, C. McCabe, S. Sarkar and K. Schmidt-Hoberg, JCAP01(2012)024, arXiv:1111.0292.
- [17] D. Hooper and C. Kelso, Phys. Rev. D **84** 083001 (2011), arXiv:1106.1066.
- [18] T. Schwetz and J. Zupan, JCAP08(2011)009, arXiv:1106.6241; C. McCabe, Phys. Rev. D **84** 043525 (2011), arXiv:1107.0741; P. J. Fox, J. Kopp, M. Lisanti and N. Weiner, Phys. Rev. D **85** 036008 (2012), arXiv:1107.0717.
- [19] J. Chervinka et al., Astropart. Phys. **35**, 749 (2012), arXiv:1106.1156.
- [20] D. N. Spergel, Phys. Rev. D **67**, 1353 (1988).
- [21] C. J. Copi, J. Heo and L. M. Krauss, Phys. Lett. B **461**, 43 (1999), astro-ph/990449; C. J. Copi and L. M. Krauss, Phys. Rev. D **63**, 043507 (2001), astro-ph/0009467.
- [22] B. Morgan, A. M. Green and N. J. C. Spooner, Phys. Rev. D **71** 103507 (2005), astro-ph/0408047.
- [23] N. Bozorgnia, G. B. Gelmini and P. Gondolo, JCAP06(2012)037, arXiv:1111.6361.
- [24] J. Billard, F. Mayet, J. F. Macias-Perez and D. Santos, Phys. Lett. B **691**, 156 (2010), arXiv:0911.4086.
- [25] A. M. Green and B. Morgan, Phys. Rev. D **81**, 061301 (2010), arXiv:1002.2717.
- [26] B. Morgan and A. M. Green, Phys. Rev. D **72**, 123501 (2005), astro-ph/0508134.
- [27] A. M. Green and B. Morgan, JCAP08(2007)022, astro-ph/0609115.
- [28] G. Sciolla and C. J. Martoff, New J. Phys. **11** 105018 (2009), arXiv:0905.3675.
- [29] S. Ahlen et al., Int. J. Mod. Phys. A **25** 1-51 (2010), arXiv:0911.0323.
- [30] G. Sciolla et al., J. Phys. Conf. Ser. **179** 012009 (2009), arXiv:0903.3895; S. Ahlen et al., Phys. Lett. B **695**, 124 (2011), arXiv:1006.2928; J. B. R. Battat et al., arXiv:1109.3270.
- [31] D. P. Snowden-Ifft, C. J. Martoff, and J. M. Burwell, Phys. Rev. D **61**, 1 (2000), astro-ph/9904064; G. J. Alner et al., Nucl. Inst. and Meth. A. **535**, 644 (2004); E. Daw et al., arXiv:1110.0222.
- [32] D. Santos et al., J. Phys. Conf. Ser. **309** (2011) 012014, arXiv:1102.3265.
- [33] T. Tanimori et al., Phys. Lett. B **578**, 241 (2004) astro-ph/0310638; K. Miuchi et al., Phys. Lett. B **686**, 11 (2010), arXiv:1002.1794; K. Miuchi et al., 1109.3099.
- [34] J. Billard, F. Mayet and D. Santos, JCAP04(2012) 006, arXiv: 1202.3372.
- [35] C. J. Copi, L. M. Krauss, D. Simmons-Duffin and S. R. Stroiney, Phys. Rev. D **75**, 023614 (2007), astro-ph/0508649.
- [36] J. Billard, F. Mayet and D. Santos, Phys. Rev. D **85**, 035006 (2012), arXiv:1110.6079.
- [37] M. S. Alenazi and P. Gondolo, Phys. Rev. D **77** 043532

- (2008), [arXiv:0712.0053](#).
- [38] A. M. Green and B. Morgan, *Phys. Rev. D* **77** 027303 (2008) (4 pages), [arXiv:0711.2234](#).
- [39] M. C. Smith et al., *Mon. Not. Roy. Astron. Soc.* **379**, 755 (2007), [astro-ph/0611671](#).
- [40] P. J. McMillan and J. J. Binney, *Mon. Not. Roy. Astron. Soc.* **402** 934 (2010), [arXiv:0907.4685](#).
- [41] M. Brhlik and L. Roszkowski, *Phys. Lett. B* **464**, 303 (1999), [hep-ph/9903468](#).
- [42] A. M. Green, *JCAP10(2010)034*, [arXiv:1009.0916](#).
- [43] J. March-Russell, C. McCabe and M. McCullough, *JHEP05(2009)071*, [arXiv:0812.1931](#).
- [44] C. McCabe, *Phys. Rev. D* **82** 023530 (2010), [arXiv:1005.0579](#).
- [45] C. Savage, K. Freese, P. Gondolo and D. Spolyar, *JCAP09(2009)036*, [arXiv:0901.2713](#).
- [46] M. Kamionkowski and A. Kinkhabwala, *Phys. Rev.* **57** 3256 (1998), [hep-ph/9710337](#).
- [47] M. Lisanti, L. E. Stigari, J. G. Wacker and R. H. Wechsler, *Phys. Rev. D* **83** 023519, [arXiv:1010.4300](#).
- [48] M. Farina, D. Pappadopulo, A. Strumia and T. Volansky, *JCAP11(2011)010*, [arXiv:1107.0715](#).
- [49] P. S. Behrozzi, A. Loeb and R. H. Wechsler, [arXiv:1208.0334](#).
- [50] R. Schoenrich, J. Binney and W. Dehnen, *Mon. Not. Roy. Astron. Soc.* **403**, 1829 (2010), [arXiv:0912.3693](#).
- [51] M. Fairbairn and T. Schwetz, *JCAP01(2009)037*, [arXiv:0808.0704](#).
- [52] M. Vogelsberger et al., *Mon. Not. Roy. Astron. Soc.* **395**, 797 (2009), [arXiv:0812.0362](#).
- [53] M. Kuhlen et al., *JCAP02(2010)030*, [arXiv:0912.2358](#).
- [54] C. S. Kochanek, *Astrophys. J* **457**, 228 (1996).
- [55] M. Lisanti and D. N. Spergel, [arXiv:1105.4166](#); M. Kuhlen, M. Lisanti and D. N. Spergel, [arXiv:1202.0007](#).
- [56] C. W. Purcell, A. R. Zentner and M-Y Wang, [arXiv:1203.6617](#).
- [57] A. Natarajan, C. Savage and K. Freese., *Phys. Rev. D* **84** 103005 (2011), [arXiv:1109.0014](#).
- [58] A. M. Green and B. Morgan, in preparation.
- [59] Various talks at ‘CYGNUS 2011: 3rd Workshop on directional detection of Dark Matter’, <http://lpsc.in2p3.fr/Indico/conferenceTimeTable.py?confId=466#20>
- [60] D. Santos et al. [arXiv:1111.1566](#).
- [61] S. Burgos et al., *JINST* **4** P04014 (2009), [arXiv:0903.0326](#).
- [62] D. P. Finkbeiner, T. Lin and N. Weiner, *Phys. Rev. D* **80**, 115008, [arXiv:0906.002](#); M. Lisanti and J. G. Wacker, *Phys. Rev. D* **81** 096005 (2010), [arXiv:0911.1997](#).
- [63] G. S. Watson, *Geophys. Suppl. Mon. Not. Roy. Astron. Soc.* **7**, 160 (1956).
- [64] G. S. Watson, *Statistics on Spheres*, Wiley, New York (1983).
- [65] K. V. Mardia and P. Jupp, *Directional Statistics*, Wiley, Chichester (2002).
- [66] M. A. Stephens, *J. Amer. Statist. Assoc.* **59**, 160 (1964).
- [67] G. S. Watson, *J. Geol.* **74**, 786 (1966).
- [68] C. Bingham, *Ann. Stat.* **2**, 1201 (1974).